Journal of Renewable Energy and Environment

Research Article

Journal Homepage: www.jree.ir

The Effect of Aperture Size on the Cavity Performance of Solar Thermoelectric Generator

Mohammad Ameri* , Omid Farhangian Marandi, Behrouz Adelshahian

Department of Mechanical and Energy Engineering, Shahid Beheshti University, Tehran, Iran.

PAPER INFO

Paper history:
Received 29 March 2018
Accepted in revised form 10 September 2018

Keywords:
Cavity Receiver
Thermoelectric Generator
Heat Transfer
Aperture Size

ABSTRACT

In this manuscript, a solar cavity packed with the thermoelectric generator modules has been investigated numerically. The hot plate of TEG modules makes the inner surface of the cube, and the cold plate is the outside the cavity, under natural convection. The TEG modules are electrically in series. The solution algorithm using the equations of heat transfer and generated power of TEG modules is developed via MATLAB and simulated under various non-concentrated irradiation levels. The variation of generated power in solar thermoelectric cavity shows that increasing of the solar irradiance caused increasing the growing rate of the generated power. The radiation varies from 700 to 1200 W/m^2, and the generated power is increased from 0.26 mW to 10 mW in the side of TEGs and up to 30 mW in the bottom of TEGs. The evaluation of aperture size indicates although the generated power of fully open cavity is 2.25 times higher than the generated power in 0.05×0.05 m^2 aperture size cavity, its efficiency is 46% lower than the small aperture cavity. Heat transfer analysis of cavity depicts that 91% of heat transferred by conduction in the cube surfaces. Only 6% and 3% of input energy are lost by re-radiation and convection through the aperture, respectively.

1. INTRODUCTION

The growing demands of energy and the effect of using fossil fuel resources have led to an effort to develop the new technologies for the conversion of renewable energy to electricity. One such efficient technology is the use of solar thermoelectric generators for direct conversion of solar energy into electricity, based on the Seebeck effect [1–5], which was discovered in 1836 by Thomas Johann Seebeck. Thermoelectric generators (TEGs) consist of a set of thermoelectric (TE) modules inserted between two heat exchangers. Each TE module is then composed of several tens to hundreds of pairs of TE couples connected electrically in series and thermally in parallel, which directly converts a part of the thermal energy that passes through them into electricity. The advantages of TEGs are numerous [1]:

1- Direct energy conversion;
2- No moving parts, hence no maintenance and no extra costs;
3- Noiseless operations.

The high cost has been a barrier to development of TEGs for more common applications.

*Corresponding Author's Email: ameri_m@yahoo.com (M. Ameri)

The conversion efficiency of TEGs strongly depends on the figure of merit (ZT) and the temperature difference between the hot and cold plates as described by the equation (1) [5]:

$$\eta = (1 - T_c/T_h)\left(\frac{\sqrt{1+ZT}}{\sqrt{1+ZT}+T_c/T_h}\right) \quad (1)$$

Where η is the conversion efficiency of heat to electricity, T_c and T_h are the temperatures of cold and hot sides of a TEG, respectively.

There are many methods for classifying TE materials, one of which is based on the temperature [6]. Therefore, TE materials can be divided into three sections. At the high temperatures (800-1300 K), ceramics like $BaUO_3$ (ZT=) and semiconductors like SnSe single crystal (ZT=2.6±0.3) can be used [7, 8]. At the middle temperatures (300-800 K), semiconductors like $Bi_2Te_{2.85}Se_{0.15}$ (ZT=2.38) can be used [9]. At the low temperatures (200-400 K), semiconductors like Bi_2Te_3 (ZT=2.4) [10] and at room temperature polymers like ethylene dioxythiophene (ZT=0.4) can be used [11]. It is said that ZT must be greater than 3 to compete with a traditional generator.

The basic idea of solar thermoelectric generators (STEGs) is applying the heat of sun as a heat source for the hot side of TEGs. Different options can be used [1]:

- Directly concentrate the solar flux received by optical concentrators or by using classical solar concentrators,
- Use of the TEG as a heat exchanger in a CHP system

The efficiency of the first developed STEG was less than 1% [12].

However, due to the rapid advances of material science, STEGs are applied in different solar systems. These systems can be classified into four types: (i) Non-concentrated STEGs, (ii) Concentrated STEGs, (iii) Thermal TEG hybrids and (iv) Photovoltaic TEG hybrids [13].

Before the 1990s, thermoelectric devices mainly consisted of the bulk thermoelectric materials and showed little improvements. In 2011, Kraemer et al. [14] developed a promising flat-panel STEG with several times high efficiency. Baranowski et al. [15] showed the total efficiency of current TE materials could be 14.1% with a hot side temperature of 1273.15 K and a solar intensity concentration of 100 and including a non-ideal optical system. Chen et al. [16] and Kossyvakis et al. [17] also conducted calculations to optimize STEG design.

He et al. [18, 19] explored the coupling of solar water heating with a TEG. The experimental prototype unit was based on a solar concentrator with the glass evacuated tubes. The heat-pipe transferred the absorbed solar heat within the glass evacuated tube to a water channel. The TEG worked as a heat exchanger between the heat pipe and the water channel. Although the electrical efficiency was low (about 1 to 2%), the overall efficiency must be taken into account but as it was a CHP system. The efficiency of the produced hot water was quite good (about 55%).

Chavez et al. presented a solar hybrid electrical/thermal system with a radiation concentrator. The concentrator illuminated a TEG which was cooled by a thermosiphon providing hot water. The system generated 20 W of electrical energy and 200 W of thermal energy stored in water with a temperature of around 323 K [20, 21].

Many researchers used the TEG modules in the heat recovery systems such as photovoltaic-thermoelectric hybrid systems. Soltani et al. tested a photovoltaic-thermoelectric hybrid system at the different cooling conditions. Natural cooling, air forced cooling, water cooling and nanofluid cooling were applied for enhancing the heat transfer of the TEG cold plate. The tests showed that using nanofluid cooling had remarkable better results for the total power of the hybrid system comparing to the air cooling methods [22]. A hybrid photovoltaic thermoelectric system at the concentrated solar irradiance by applying Fresnel lens and water heat extracting unit was studied by Willars-Rodríguez et al. [23]. This hybrid system could reach to the electrical efficiency of 20% and thermal efficiency of 40%. The three-dimensional numerical model of the perovskite PV-TEG hybrid system had been studied and, the results showed that the temperature coefficient of the perovskite solar cell was lower than 2% K^{-1}. The low-temperature coefficients caused the efficiency of 18.6% [24].

A heat transfer analysis of directly irradiated single TEG modules has shown that 60% of the incident solar radiation was lost by re-radiation [25]. Experimental study of the TEG cavity configuration showed that using enclosure caused reduction of the re-radiation losses from 60% to 4% of the concentric solar radiative power input [26].

Based on the previous studies, the effective parameters on the STEG performance are the thermoelectric materials, figure of merit and the application of optimized thermal heat source. The high performance materials are in the development stage in the laboratory conditions and are not economical for industrial scales. Therefore, this paper is focused on the radiation gathering from sunlight to improve the thermoelectric hot plate heat absorption by reducing re-radiation loss. The heat transfer analysis of thermoelectric cavity system under non-concentrated solar irradiation is investigated and the related equation coupled with the electrical power generation equation is analyzed. The effect of the aperture size on the power generation and efficiency of the solar cavity is studied, and contribution of conduction, convection and re-radiation is shown in this system configuration.

2. HEAT TRANSFER MODEL

The configuration of solar cavity receiver is showed schematically in Fig. 1. It consists of a cubic box with a square aperture for the access of input irradiation. Smaller apertures reduce re-radiation losses but intercept less sunlight. On the other hand, fully open cavities intercept more irradiation and also more losses.

The cavity contains 4 TEG devices on the every side. The conduction heat transfer through the thermoelectric legs is 1D. The heat transfer modes within the cavity are radiation and natural convection exchange. Moreover, the following assumptions are considered: (1) the TEG surfaces are opaque, gray and diffuse; (2) the TEG module has uniform temperatures; (3) the inside air of the cavity is non-participating media, and (4) the TEGs are simulated in the ideal form.

Radiation heat exchange is solved by the radiosity method [27], yielding a system of equations regarding the net radiative fluxes and the temperatures as equation (2):

$$\varepsilon_k \,.\, \sigma \,.\, T^4 = \sum_{j=1}^{N} \left[\delta_{k\,j} - (1 - \varepsilon_k) \,.\, F_{k-j} \right] \,.\, q_{o,j} \qquad (2)$$

Where ε, σ, T, F and q_o are the surface emissivity, the constant of Stefan–Boltzmann, the surface temperature, view factor and radiosity flux, respectively.

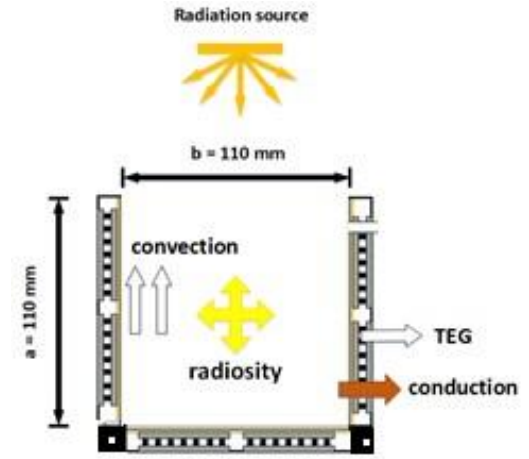

(a)

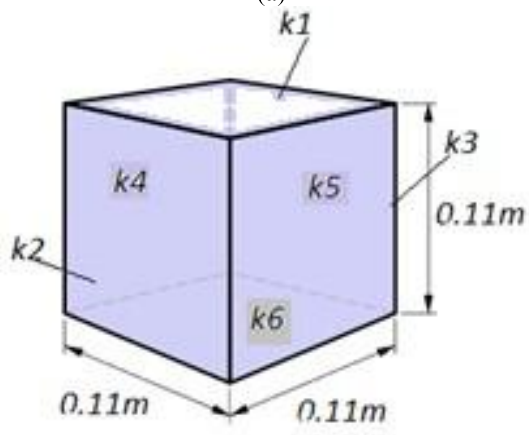

(b)

Figure 1. (a) Schematic of the solar thermoelectric cavity model domain (b) overall dimension and surface No. of the cavity

By considering the convection inside the cavity, the conduction through the cavity wall is lead to equation (3) as follow:

$$\frac{Q_{cond}}{A_k} + q_{solar} - q_{conv} = \sum_{j=1}^{N}\left[\delta_{kj} - F_{k-j}\right].\ q_{o,j} \quad (3)$$

Where, Q_{cond}, q_{conv} are conduction heat transfer through the wall and the cavity wall of convection heat transfer. The cavity is discretized into 6 radiating surface elements. The view factors of F_{k-j} are calculated by applying reciprocity relations $A_j.F_{j-k}=A_k.F_{k-j}$, enclosure criterion $\sum_{j=1}^{N} F_{k-j} = 1$, and tabulated view factors for parallel and perpendicular plates [28].
Based on [29], the convective heat transfer coefficient is defined as the equation (4):

$$Nu = \exp(-1.736 + 0.34 * ln(Ra)) \quad (4)$$

Where Nu is the Nusselt number and Ra is the Rayleigh number which calculated as equation (5):

$$Ra = .\frac{g.\beta}{\vartheta.\alpha}(T_{wall} - T_{air}).L^3 \quad (5)$$

Where g, β, ν, α, T_s, T_∞ and L are gravitational acceleration, the coefficient of thermal expansion, kinematic viscosity, thermal diffusivity, the surface temperature, the air stream temperature and characteristic length-scale of convection, respectively.
The air properties in the air film temperature are calculated as equations (6) and (7) [30]:

$$k_{air} = \frac{3.14*10^{-4}.{k_{air}}^{0.7786}}{1-\frac{0.7116}{T_{air}}+\frac{2121.7}{{T_{air}}^2}} \quad (6)$$

Where k_{air} is air conductivity and

$$\mu_{air} = \frac{1.425*10^{-6}.T^{0.5039}}{1+\frac{108.3}{T_{air}}} \quad (7)$$

In which, μ_{air} is the air dynamic viscosity.
So, the convective heat transfer inside the cavity is calculated by (8):

$$q_{conv} = h.(T_{1,k} - T_{air,in}) \quad (8)$$

The temperature of the hot and cold side of the TEG can be found by (9):

$$T_{2,k} = T_{1,k} - R_{TEG}\,.\,q_{cond} \quad (9)$$

The system of equations is solved together via MATLAB for different values of solar irradiation (700-1200 W/m^2) and an ambient air temperature of 298 K. The cavity surface in starting point is assumed 298 K. Then, the maximum power output from the TEGs can be found as equation (10) according to the temperature values of the different points in the cavity and radiation distribution on each surface [2]:

$$P_{TEG,max} = \frac{1}{4}\frac{V_{TEG}^2}{R_{TEG}} \quad (10)$$

Where, $P_{TEG,max}$, R_{TEG}, and V_{TEG} are the maximum generated power by the TEG, the internal electrical resistance and the open circuit of TEG module, respectively. Also, V_{TEG} is calculated by equation (11):

$$V_{TEG} = S.(T_{1,k} - T_{2,k}) \quad (11)$$

Where, S is the Seebeck coefficient, and $T_{1,k}$ and $T_{2,k}$ are the temperatures of the hot and cold plate of the k^{th} surface. The modeling parameters are listed as Table 1:

TABLE 1. Modeling Parameters

Parameters	Value
ε_k	0.8
σ	5.669×10^{-8} W/m^2·K^4
L	0.11 m
R_{TEG}	2.6 K/W
S	0.05 V/K
$T_{1,k}$ and $T_{2,k}$	298 K at the surface k=2-5 and t=0 0 K at the surface k=1 and t=0
q_{cond}	0 *insulation condition* at the surface k=2-5 and t=0

3. RESULTS AND DISCUSSION

3.1. PV and TEG specification

The specification of the considered TEG module is presented in Table 2.

TABLE 2. TGM-127-1 module specifications

Parameter	Symbol	Value
Width	W (mm)	40
Length	L (mm)	40
Height	H (mm)	4.8
Maximum voltage	V_{max} (V)	3.6
Maximum current	I_{max} (A)	1.23
Maximum power	P_{max} (W)	4.5
Efficiency	η (%)	5.4
Electrical resistance	R_{elec} (Ω)	3
Thermal resistance	R_{th} (K/W)	2.6

3.2. Validation of the numerical method

For validation of the numerical model, the results have been compared with TEG cavity results which were investigated experimentally by Suter et al. [26]. They studied the cavity in the laboratory conditions of simulated irradiation. The temperature of all surface and generated power are reported in the reference of [26]. The experimental and theoretical simulations results are shown in Table 3. The difference of the experimental and theoretical simulations are less than 8% in the generation of the electrical power and the calculation of the temperature , which confide that the model can be used to simulate the TEG cavity system.

TABLE 3. Comparison between numerical and experimental data

Parameters	Numerical	Experimental[26]	Error
Downside Temperature	887 K	847 K	4%
Side Temperature	722 K	679 K	6.3%
Efficiency	0.129 %	0.12 %	7.4%

3.3. Fully open STEG cavity numerical study

The temperature difference between T_1 (Hot plate temperature) and T_2 (Cold plate temperature) is the gradient through the TEG module, which causes power generation by the TEG module. Fig. 2 shows the hot and cold plate temperature of the bottom face of TEG modules under the different level of the irradiation and natural convection of outside air. Fig. 2 depicts higher irradiance leads to a higher temperature difference through the TEG and, consequently, more output power.

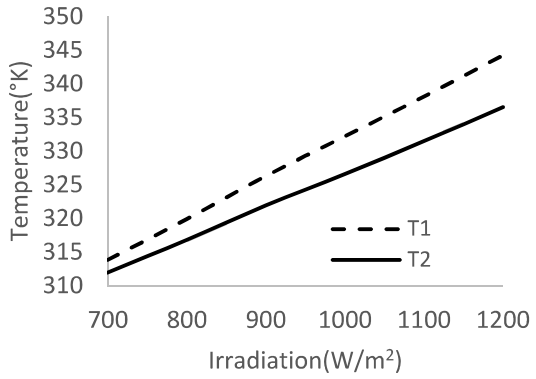

Figure 2. The variation temperature of hot and cold plate of TEG in the bottom face under various solar radiation levels

The comparison between the temperatures of side face and bottom side of TEG is showed in Fig. 3. The temperature of the side face of TEG is raised by increasing the irradiation level. The bottom face temperature is more than side face, because the bottom face is exposed to main part of input irradiation and re-radiation from the cavity walls, which is shown in Fig. 3.

Fig. 4 (a) and (b) show the thermoelectric generators of open circuit voltage and current, respectively. As a consequence of the higher temperature difference in the

bottom face, the voltage and current of the bottom face are higher than the side face of thermoelectric generators.

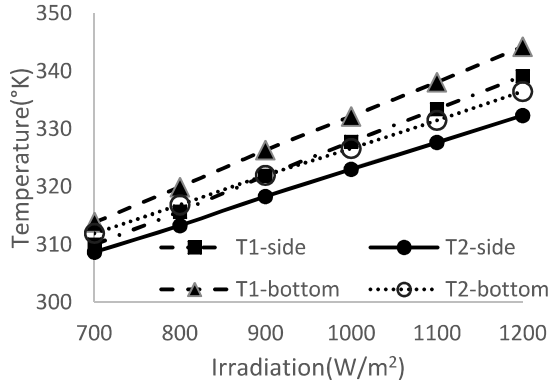

Figure 3. The temperature comparison between hot and cold plate of TEG in the bottom face and side face of the cavity

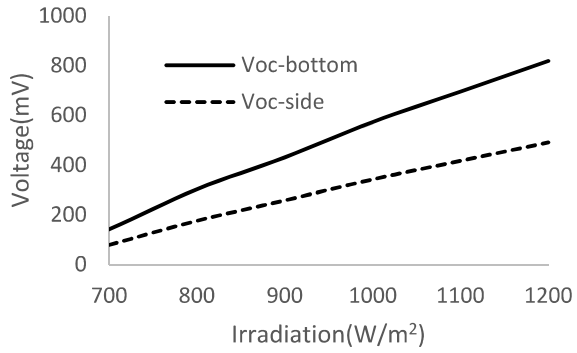

(a)

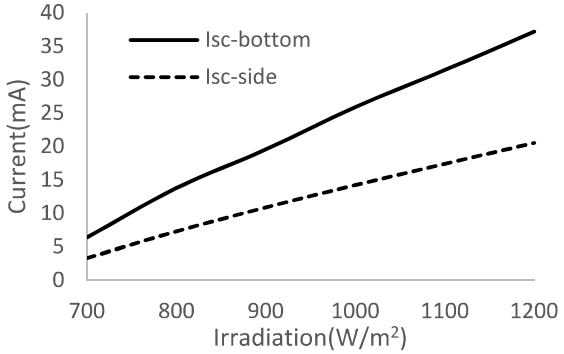

(b)

Figure 4. (a) The open-circuit voltage and (b) short- circuit voltage of the side and bottom face of TEGs

The power variation in the solar thermoelectric cavity is shown in Fig. 5. The radiation varies from 700 to 1200 W/m^2, and the generated power increases from 0.26 mW to 10 mW for the side of TEGs, and up to 30 mW for the bottom side of TEGs. This irradiation is normal radiation on the cavity aperture and it is assumed that the light angle is perpendicular to aperture surface. In real condition, the sunlight angle changes during times of a day and it is necessary to track the sunlight to reach the peak of generation power in all times of a day. On the other hand, the sun tracking mechanism increases the cost of the produced electricity and so for different environment and sunlight level conditions, and the best method should be technically and economically analyzed.

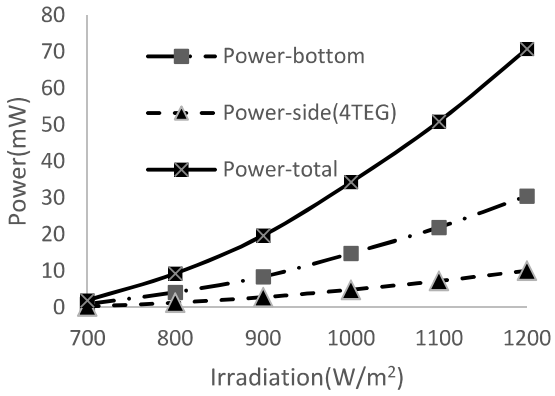

Figure 5. The fully open cavity generated power variation under various solar radiation levels

3.4. STEG cavity aperture size effect

It is possible to change the size of the cavity aperture from fully close to fully open aperture size that is 0.11×0.11m^2 in this study. The effect of the reduction of aperture size on the cavity power generation and the re-radiation loss from the aperture is studied for aperture size of 0.05×0.05 m^2.

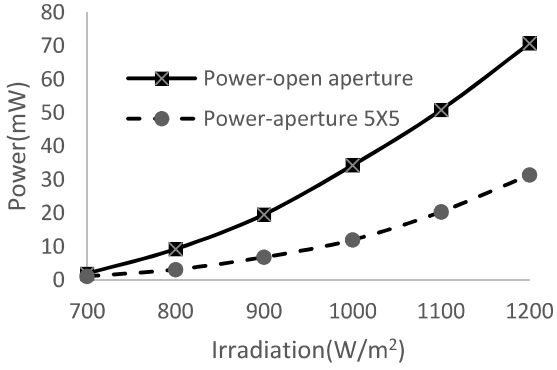

Figure 6. Power generation of the cavity with the aperture size of 0.05×0.05 m^2 for different radiation levels

The comparison of the maximum generated power by TEG modules in the cavity with the aperture size of 0.05×0.05 m^2 in different irradiation levels and the fully open cavity is shown in Fig. 6. Although reducing the aperture size causes the decreasing of the re-radiation,

reduction of input power causes the decreasing of the generated power. Comparison of two cases in 1000 W/m^2 shows that the generated power in the fully open cavity is 2.25 times more than generated power in 0.05×0.05 m^2 aperture size cavity.

The comparison of the solar thermoelectric cavity efficiency in the fully open and the reduced size aperture condition is presented in Fig. 7. The analysis of Figs. 6 and 7 depict that despite the reduction of output power, the cavity with smaller aperture size is more efficient than the fully open cavity. The re-radiation losses of cavity aperture are decreased by reducing the aperture size and the efficiency of the system is increased.

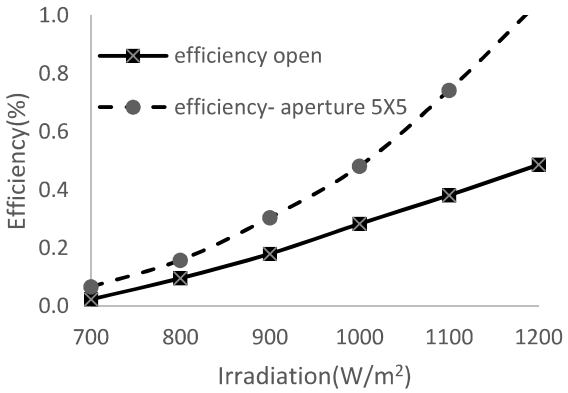

Figure 7. Solar thermoelectric cavity efficiency for different radiation levels

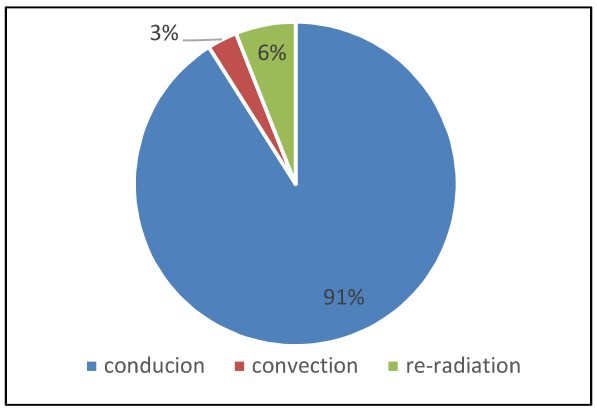

Figure 8. The percentage of the transferred heat in the cavity receiver Q_{solar}=1000 w/m^2 with the aperture size of 0.05×0.05 m^2

The main concern of the electricity production in the thermoelectric generator is the temperature difference. Therefore, for TEG systems using cavities without any concentrating tools, it is recommended to harvest the radiation by having active cooling systems such as air blowers on the backside of the TEG modules. The effect of using STEG cavity system by active cooling on the cost of produced electricity should be studied and the best economic and technical method should be proposed.

The corresponding percentages of the solar power input are transferred by the different heat transfer modes which are presented in Fig. 8. This figure shows that 91% of input solar energy is conducted through the TEG legs. Only 6% and 3% of input energy are lost by re-radiation and convection through the aperture, respectively.

4. CONCLUSIONS

In the present paper, the thermoelectric power generating system using a cubical cavity receiver is proposed and simulated via a numerical method. It is shown that higher radiation levels cause the higher temperature difference through the TEG module and leads to the higher TEG generated power. Also, another simulation is performed to evaluate the performance of the system for the aperture size of 0.05×0.05 m^2. The result showed that the reduction of obtained radiation input causes the decreasing of the mean temperature in the system. By changing the radiation from 700 to 1200 W/m^2, the generated power increases from 0.26 mW to 10 mW for the side of TEGs and up to 30 mW for the bottom side of TEGs. Heat transfer analysis of the cavity depicts that 91% of heat is transferred by conduction in cube surfaces and only 6% and 3% of input energy are lost by re-radiation and convection through the aperture, respectively.

The results depict that the re-radiation losses is decreased by applying the cavity and the system has the best performance related to absorbed solar energy. However, there are two ways for enhancing the performance of the solar thermoelectric generator performance. There are the applying of the high-performance materials which have strong effects on the cost of the device, and reducing the losses.

Studying the effect of the aperture size shows that the generated power of the fully open cavity is 2.25 times higher than the generated power in the aperture size cavity of 0.05×0.05 m^2. The maximum efficiency of the cavity with the aperture of 0.05×0.05 m^2 is 1.048%, and open aperture cavity in irradiation of 1200 W/m^2 is about 0.48% which is 50% lower than the efficiency of the small aperture cavity. The smaller aperture size reduces the re-radiation loss from aperture and cavity with smaller aperture is efficient than the fully open cavity.

Nomenclature

P	Power
A	Area
$STEG$	Solar Thermoelectric Generator
TEG	Thermoelectric Generator
ZT	Figure of Merit
F_{i-j}	View factor
g	Gravitational acceleration

L	Characteristic length-scale of convection
Nu	Nusselt number
$P_{TEG,max}$	Maximum power generated by the TEG
q_o	Radiosity flux
Q_k	Conduction heat power through the wall
R_i	Internal electrical resistance
Ra	The Rayleigh number
S	Seebeck coefficient
T_s	Surface temperature
$T_{1,k}$	Temperature of the hot plate of the kth surface
$T_{2,k}$	Temperature of the cold plate of the kth surface
k_{air}	Air conductivity

Greek symbols

μ_{air}	air dynamic viscosity
β	coefficient of thermal expansion
ϑ	kinematic viscosity,
α	thermal diffusivity
ε	surface emissivity
σ	Stefan–Boltzmann's constant
η	efficiency

8. ACKNOWLEDGEMENT

This work has been financially supported by the Grant from the Shahid Beheshti University.
This support is gratefully acknowledged.

REFERENCES

1. Champier, D., "Thermoelectric generators: A review of applications", ***Energy Conversion and Management***, Vol. 140, (2017), 167–181.
2. Rowe, DM. CRC Handbook of thermoelectric, NY, USA: CRC Press, (1995).
3. Min, G. and Rowe, D.M., Thermoelectric Handbook Macro to Nano, CRC Press, (2006).
4. Goldsmid, H.J., "Theory of Thermoelectric Refrigeration and Generation", ***Introduction to Thermoelectricity,*** Vol. 121, (2010), 7-21.
5. Hun, C., Li, Z. and Dou S.X., "Recent progress in thermoelectric materials", ***Chinese Science Bulletin***, Vol. 59, (2014), 2073-2091.
6. Li, G., Shittu, S., Diallo, T.M.O., Yu, M., Zhao, X. and Ji, J., "A review of solar photovoltaic-thermoelectric hybrid system for electricity generation", ***Energy***, Vol. 158, (2018), 41-58.
7. Kurosaki, K., Matsuda, T., Uno, S., Kobayashi, S. and Yamanaka, S., "Thermoelectric properties of $BaUO_3$", ***Journal of Alloys and Compounds***, Vol. 319, (2001), 271–275.
8. Zhao, L. D., Lo, S., Zhang, Y., Sun, H., Tan, G., Uher, C., Wolverton, C., Dravid, V.P. and Kanatzidis, M.G., "Ultralow thermal conductivity and high thermoelectric figure of merit in SnSe crystals", ***Nature***, Vol. 508, (2014), 373-377.
9. Kim, T.S., Kim, I.S., Kim, T.K., Hong, S.J. and Chun, B.S., "Thermoelectric properties of p- type $25\%Bi_2Te_3$+$75\%Sb_2Te_3$ alloys manufactured by rapid solidification and hot pressing", ***Materials Science and Engineering***, Vol. 90, (2002), 42–46.
10. Venkatasubramanian, R., Siivola, E., Colpitts, T. and O'Quinn, B., "Thin-film thermoelectric devices with high room-temperature figures of merit", ***Nature***, Vol. 413, (2001), 597–602.
11. Kim, G.H., Shao, L., Zhang, K. and Pipe, K.P., "Engineered doping of organic semiconductors for enhanced thermoelectric efficiency", ***Nature Materials***, Vol.12, (2013), 719–723.
12. Telkes, M., "Solar thermoelectric generators", ***Journal of Applied Physics***, Vol. 25, (1954), 765-777.
13. Sundarraj, P., Maity, D., Roy, S.S. and Taylor, R.A., "Recent advances in thermoelectric materials and solar thermoelectric generators–a critical review", ***RSC Advances***, Vol. 4, (2014), 46860-46874.
14. Kraemer, D., Poudel, B., Feng, H.-P., Caylor, J.C., Yu, B., Yan, X., Ma, Y., Wang, X., Wang, D., Muto, A., McEnaney, K., Chiesa, M., Ren, Z. and Chen, G., "High-performance flat-panel solar thermoelectric generators with high thermal concentration", ***Natural Material***, Vol. 10, (2011), 532–538.
15. Baranowski, L.L., Snyder, G.J. and Toberer, E.S., "Concentrated solar thermoelectric generators", ***Energy & Environmental Science,*** Vol. 5, (2012), 9055-9067.
16. Chen, W.H., Wang, C.C., Hung, C.I., Yang, C.C. and Juang, R.C., "Modeling and simulation for the design of thermal-concentrated solar thermoelectric generator", ***Energy***, Vol. 64, (2014), 287-297.
17. Kossyvakis, D.N., Vossou, C.G., Provatidis, C.G. and Hristoforou, E.V., "Computational analysis and performance optimization of a solar thermoelectric generator", ***Renewable Energy***, Vol. 81, (2015), 150-161.
18. He, W., Su, Y., Riffat, S.B., Hou, J. and Ji, J., "Parametrical analysis of the design and performance of a solar heat pipe thermoelectric generator unit", ***Applied Energy***, Vol. 88, (2011), 5083-5089.
19. He, W., Su, Y., Wang, Y.Q., Riffat, S.B. and Ji, J., "A study on incorporation of thermoelectric modules with evacuated-tube heat-pipe solar collectors", ***Renewable Energy***, Vol. 37, (2012), 142-149.
20. Chávez-Urbiola, E.A., Vorobiev, Y. and Bulat, L.P., "Solar hybrid systems with thermoelectric generators", ***Solar Energy***, Vol. 86, (2012), 369-378.
21. Chávez Urbiola, E.A. and Vorobiev Y., "Investigation of solar hybrid electric/thermal system with radiation concentrator and thermoelectric generator", ***International Journal of Photoenergy,*** Vol. 2013, (2018), 704087.
22. Soltani, S., Kasaeian, A., Sarrafha, H. and Wen, D., "An experimental investigation of a hybrid photovoltaic/thermoelectric system with nanofluid application", ***Solar Energy***, Vol. 155, (2017), 1033-1043.
23. Willars-Rodríguez, F.J., Chávez-Urbiola, E.A., Vorobiev, P. and Vorobiev, V., "Investigation of solar hybrid system with concentrating Fresnel lens, photovoltaic and thermoelectric Generators", ***International Journal of Energy Research***, Vol. 3, (2017), 377–388.
24. Zhang, J., Xuan, Y. and Yang, L., "A novel choice for the photovoltaic–thermoelectric hybrid system: the perovskite solar cell", ***International Journal of Energy Research***, Vol. 10, (2016), 1400-1409.
25. Suter, C., Tomes, P., Weidenkaff, A. and Seinfeld, A., "Heat transfer analysis and geometrical optimization of thermoelectric converters driven by concentrated solar radiation", ***Materials***, Vol. 3, (2010), 2735–2752.
26. Suter, C., Tomes, P., Weidenkaff, A. and Seinfeld, A., "A solar cavity-receiver packed with an array of thermoelectric converter modules", ***Solar Energy***, Vol. 85, (2011), 1511–1518.
27. Howell, J., Siegel, R. and Pinar, M., Thermal Radiation Heat Transfer, Fifth ed. 222- 248, New York: Taylor & Francis Inc.; (2002).

28. Catalog of Radiation Heat Transfer Configuration Factors, summary and conclusions; (2010), http:// www.me.utexas.edu/~howell/tablecon.html.

29. Hinojosa, J.F., Alvarez, G. and Estrada, C.A., "Three-dimensional numerical simulation of the natural convection in an open tilted cubic cavity", ***Revista Mexicana de Física***, Vol. 52, No. 2, (2006), 111-119.

30. Properties, D.I.F.P., DIPPR Project 801 - Full Version: Design Institute for Physical Property Research/AIChE; (2010).